



## Revealing the difference of Stark tuning rate between interface and bulk by surface-enhanced infrared absorption spectroscopy

Manyu Zhu<sup>a,b,1</sup>, Fei Liang<sup>c,1</sup>, Lie Wu<sup>a</sup>, Zihao Li<sup>a,b</sup>, Chen Wang<sup>a,b</sup>, Shule Liu<sup>c,\*</sup>,  
Xiue Jiang<sup>a,b,d,\*</sup>

<sup>a</sup> State Key Laboratory of Electroanalytical Chemistry, Changchun Institute of Applied Chemistry, Chinese Academy of Sciences, Changchun 130022, China

<sup>b</sup> School of Applied Chemistry and Engineering, University of Science and Technology of China, Hefei 230026, China

<sup>c</sup> School of Materials Science and Engineering, Sun Yat-sen University, Guangzhou 510275, China

<sup>d</sup> Research Center for Analytical Science, College of Chemistry, Nankai University, Tianjin 300071, China

### ARTICLE INFO

#### Article history:

Received 6 January 2024

Revised 4 April 2024

Accepted 30 April 2024

Available online 1 May 2024

#### Keywords:

Surface-enhanced infrared spectroscopy

Attenuated total reflection spectroscopy

Vibrational stark effect

Stark tuning rate

Cyano group

### ABSTRACT

Revealing the factors that affect the vibrational frequency of Stark probe at interface is a pre-requirement for evaluating the absolute interfacial electric field. Here using surface-enhanced infrared absorption (SEIRA) spectroscopy, attenuated total reflection (ATR) spectroscopy and molecular dynamics (MD), we reveal the assembled C≡N at gold nanofilm exhibits a reduced Stark tuning rate (STR) referring to the vibrational frequency shift in response to electric field comparing with the bulk which was regulated by the electron transfer between S and Au. These findings lead to a deeper understanding of the vibrational Stark effect at the interface and provide guidance for improving the interface electric field theory.

© 2024 Published by Elsevier B.V. on behalf of Chinese Chemical Society and Institute of Materia Medica, Chinese Academy of Medical Sciences.

Interface is an important aspect of chemistry on which many enzyme-catalyzed and electrochemistry reactions all take place [1,2]. Electrochemical interfaces involving electrodes/electrolytes are not only the most common interfaces, but also typical models for studying interfacial reactions [3,4]. The promotion or suppression of the electrochemical reaction can be modulated by changing the electrode potential [5-7], but it is worth noting that the interfacial electric field itself exists intrinsically which would inevitably affect the progress of the reaction at the interface. The composition, charge, polarity, solvent properties, and hydrated ions at the interface will all affect the interface electric field [7-10] which has brought greater difficulty to the challenging direct measurement of interfacial electric field. An accurate and quantitative description of the interface electric field is of great significance for revealing the underlying biological and chemical reaction mechanism, and it is also a great challenge in the study of the interfaces.

Vibrational Stark effect (VSE) describes a molecular vibration that is sensitive to the local electrostatic field will show a field-induced change in the vibrational frequency and spectral intensity [11], which provides a direct way to measure local electric field by employing a molecular probe having polar bonds [12]. Nitrile

group (CN) has attracted extensive attention as a VSE probe to indicate changes in the local electric field due to its large dipole moment and the distinguished absorption band from most studied functional groups [13], which have been used to detect the electric field in the active site of enzyme [14] and the distribution across the electric double layer of electrode/electrolyte interfaces [15]. This method is based on the calibration between the vibrational frequency shift of the probe and the electric field applied either by an electrode or by surrounding solvent with different dielectric constant [16,17]. It is worthy to note that the experimental vibrational frequency shift can be derived from factors other than VSE that would interfere with the accurate assessment of the electric field [18,19] which may cause the misjudgment of the electric field. Hence it is the urgent task to reveal the factors that affect the frequency shift of the stark probe at the interface.

Surface-enhanced infrared absorption (SEIRA) spectroscopy is an exquisitely surface sensitive technique by taking advantage of enhancement and near-field effect of nanostructure metal film, resulting an enhancement factor of 10–1000 for molecules adsorbed to the metal film and the decay of the enhanced signal within 10 nm (Fig. 1a) [20,21], while attenuated total reflection (ATR) spectroscopy detects the characteristics of the bulk because the penetration depth of the evanescent wave generated in the ATR mode is about 0.5–2 μm (Fig. 1b) [22]. 4-Mercaptobenzonitrile (MBN) is a widely used probe for reporting local electric fields in the study of electrode/solution interface [17,23] because it can

\* Corresponding authors.

E-mail addresses: liushle@mail.sysu.edu.cn (S. Liu), jiangxiue@ciac.ac.cn (X. Jiang).

<sup>1</sup> These authors contributed equally to this work.

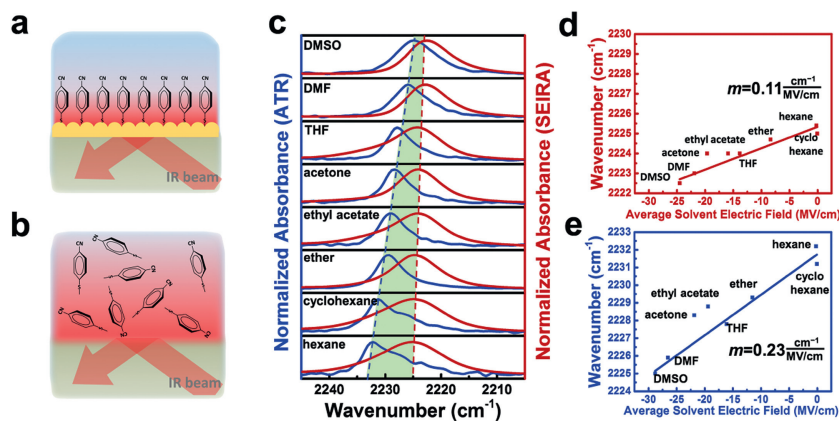


**Fig. 1.** (a, b) Diagram of MBN at interface and in the bulk. (c) ATR spectra (blue line) and SEIRA spectra (red line) of MBN in solvents with different polarity. SEIRA spectra (d) and ATR spectra (e) of the CN vibration plotted as a function of the local electric field obtained by calculation. The slope,  $m$  is  $f$ STR, where  $f$  (the local field correction factor) is a scalar estimated to be  $\sim 2$ .

be directly attached to the metal through the sulfhydryl group with uniform adsorption orientation and the conjugated structure of the benzene ring makes CN sensitive to the changes in electronic structure [23]. Applying these methods combining with solvatochromism and molecular dynamics (MD) simulations, we reveal the difference in Stark tuning rate (STR) between the bulk solution and the interface referring to experimental vibrational frequency change with a local electric field which is different from intrinsic STR referring to the difference dipole moment of the bond between the ground and excited vibrational states in the presence of an external electric field. We found that the decrease of STR at interface was not only due to the reduced solvation reaction field at the interface but also induced by electron transfer between S atom of sulfhydryl molecule and Au nanofilm. Our research reveals the multiple reasons for the reduction of the STR at the interface and lay a foundation for better understanding the interfacial VSE and evaluation of local electric field.

SEIRA and ATR spectra of MBN were recorded at  $1 \text{ cm}^{-1}$  resolution with 512 scans after taking different solvents as background spectrum to measure the vibrational response of MBN at interface and in the bulk. As shown in Fig. 1c, the characteristic absorption peak attributed to  $\nu(\text{C}\equiv\text{N})$  of MBN between  $2150 \text{ cm}^{-1}$  to  $2300 \text{ cm}^{-1}$  exhibits a more pronounced red shift at interface (red curves) than in the bulk (blue curves) which might reflect the fact that CN experiences different electric fields and/or CN exhibits different STR in these two modes. To understand how the magnitude of electric field around the CN varies in different systems, we performed MD simulations to calculate the ensemble-averaged electric field of different kinds of solvents in the bulk and at interface, respectively (Tables S2 and S3 in Supporting information). As reported, the interfacial electric field is slightly smaller than the bulk due possibly to an extra electric field induced by metal image dipole when bonding of MBN with gold interface [17]. Nevertheless, the STR of MBN at the interface ( $0.055 \text{ cm}^{-1}/(\text{MV}/\text{cm})$ , Fig. 1d) is still smaller than that in the bulk ( $0.115 \text{ cm}^{-1}/(\text{MV}/\text{cm})$ , Fig. 1e), suggesting that the sensitivity of the MBN frequency to local electric field at the interface is lower than that in the bulk free state, that is, relative to the bulk, after assembling at interface, the same electric fields along the CN induces a smaller change in its vibrational frequency. Discovering the origin of the difference can help us to better understand the interfacial VSE.

The intermolecular interaction may influence the electron structure, which in turn affects infrared vibration wavenumber further affects its STR.  $\pi$ - $\pi$  interaction is an intrinsic interaction caused by intermolecular overlapping of p-orbital in  $\pi$  conjugated molecules containing aromatic groups [24]. In order to explore whether there is a difference in  $\pi$ - $\pi$  interaction of MBN at interfacial assembly

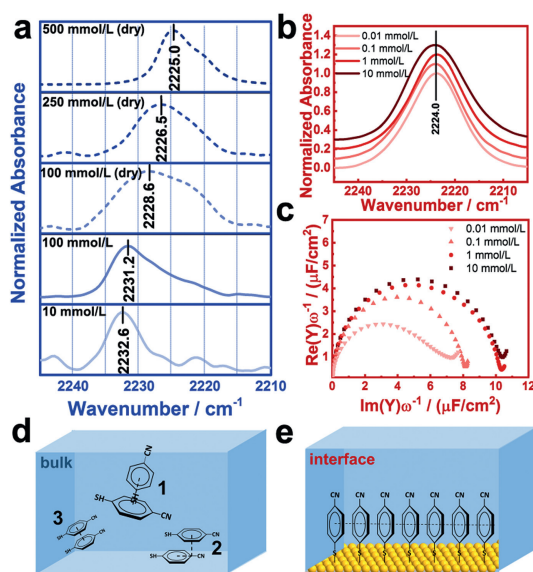


**Fig. 2.** (a) The ATR spectra of MBN with different concentrations. (b) The SEIRA spectra of MBN with different concentrations. (c) EIS measurements of MBN SAM with different concentrations on nanostructured Au electrodes. (d, e) Diagram of  $\pi$ - $\pi$  interaction of MBN in the bulk and at interface.

state and in the bulk, considering the stacking effect strengthens with the increase of the concentration and will lead to a red shift of characteristic absorption peak in the infrared spectrum [25], we monitored the ATR spectra of MBN with different concentrations. Although with the decrease of concentration, the signal-to-noise ratio gets worse after normalization, the characteristic absorption peak of CN still can be clearly identified (Fig. 2a). As the concentration gradually increased from 10 mmol/L to 50 mmol/L and finally to 100 mmol/L, the band of CN exhibits a red shift from  $2232.6 \text{ cm}^{-1}$  to  $2232.2 \text{ cm}^{-1}$  and finally to  $2231.2 \text{ cm}^{-1}$  (Figs. 1c and 2a), indicating the enhancement of intermolecular  $\pi$ - $\pi$  interaction. To further verify  $\pi$ - $\pi$  interaction induces the red shift of CN, we recorded the spectra dried with Ar stream after taking Si prism exposed in air as the background spectrum. The removal of solvent makes MBN tend to arrange like a stack of coins, so we observed  $2.6 \text{ cm}^{-1}$  red shift (from  $2231.2 \text{ cm}^{-1}$  to  $2228.6 \text{ cm}^{-1}$ ) of CN after solvent removal in 100 mmol/L MBN, and it further red shifts with the increasing concentration. The appearance of shoulder peak after drying solvent may come from MBN clusters of different sizes [25]. Notably, when different concentrations of MBN were assembled on Au nanofilm, the band of CN remained

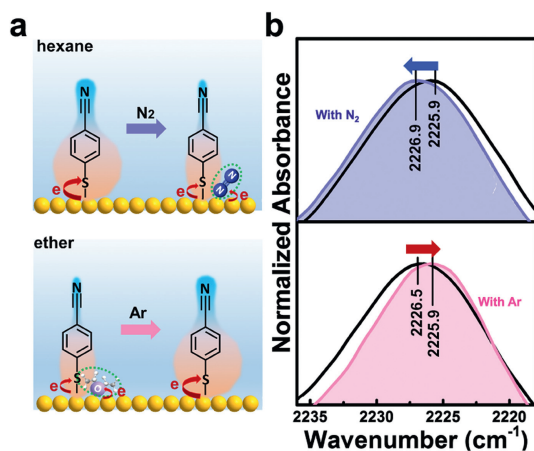


**Fig. 3.** (a) Diagram of electron transfer between S and Au in hexane (top panel) and ether (bottom panel). The green dot circles represent N<sub>2</sub> (top panel) and ether (bottom panel), respectively. (b) The corresponding SEIRA spectra of MBN in hexane with (purple line)/without (black line) N<sub>2</sub> stream (top panel) and SEIRA spectra of MBN in ether with (pink line)/without (black line) Ar stream (bottom panel).

unchanged at 2224.0 cm<sup>-1</sup> (Fig. 2b). To explore whether it roots in the adsorption saturation of MBN at interface or in the unchanged  $\pi$ - $\pi$  interaction after assembling in different concentrations at interface, electrochemical impedance spectroscopy (EIS) was used to characterize the formation of self-assembled monolayer (SAM) [26]. As shown in Fig. 2c, the interfacial capacitance varies with SAMs assembled in different concentrations, implying the unsaturated adsorption of MBN at interface. Consequently, the constant absorption peak of CN should result from unchanged  $\pi$ - $\pi$  interaction among MBN after assembling in different concentrations at interface. According to the orientation of the aromatic ring, the  $\pi$ - $\pi$  interaction between aromatic molecules can be roughly divided into three prototype configurations [27]: Edge to face T-shaped configuration (Fig. 2d-1), parallel-displaced configuration (Fig. 2d-2) and sandwich configuration (Fig. 2d-3) with gradually decreased stability [28]. When MBN is dispersed in the bulk with free orientation, they prefer T-shaped configuration between molecules [29,30] rather than the other two configurations, resulting in stronger  $\pi$ - $\pi$  interaction while only sandwich configuration exists at interface (Fig. 2e) due to the fixed orientation caused by the formation of Au-S bonding. The interaction between molecules causes the migration of the electron cloud and then induces the shift of the absorption band in the infrared spectrum. As for  $\pi$ - $\pi$  interactions mentioned above, the quadrupole-quadrupole interaction is attractive for the T-shaped and parallel-displaced configurations, while is repulsive for sandwich configuration [31]. Therefore, the equilibrium of repulsive forces between adjacent molecules does not change the electron cloud distribution, so it shows the same characteristic absorption peak position. Theoretically, if  $\pi$ - $\pi$  interaction causes the difference between interface and bulk, SEIRA spectra of CN in MBN should be blue-shifted relative to ATR spectra due to weaker  $\pi$ - $\pi$  interaction, which is contrary to what we have observed experimentally, so it is not the case.

The most intuitive difference between interface and the bulk is the formation of the Au-S bond. When S atom bonds to Au, there's electron flow from Au to S [32] possibly because S is more electronegative than Au which is similar to that more electronegative atoms are more likely to act as electron acceptors [33] which affects the electronic structure of the whole molecule and further induces vibrational frequency shift. Analogously, oxygen-containing species can easily interact with Au due to its higher electronegativity (3.44) comparing with Au (2.54) which interferes the electron transfer between S and Au and further induced vibrational wavenumber shift. To verify this speculation, we recorded sample

spectra of MBN assembled in hexane and ether and then dried with air stream after taking Au nanofilm exposed in air as the background spectrum (Fig. 3a). As shown in Fig. 3b, the band of CN in ether shows the maximal absorption at 2226.5 cm<sup>-1</sup> (black line in bottom panel), which is blue shifted by 0.6 cm<sup>-1</sup> (from 2225.9 cm<sup>-1</sup> to 2226.5 cm<sup>-1</sup>) comparing with that in hexane (black line in top panel), resulting from the reduction of electron transfer between S and Au due to the interaction between the O atom of gaseous ether and Au. Hence, we speculate that the occurrence of electron transfer between S and Au contributes to the vibrational wavenumber of CN which makes it differ from that in the bulk. In order to prove it, we dried with N<sub>2</sub> instead of air stream due to its higher electronegativity (3.04) to obtain sample spectra under the reduction of the electron transfer between S and Au (Fig. 3b, purple line in top panel), CN vibration undergoes a blue shift of 1.0 cm<sup>-1</sup> (from 2225.9 cm<sup>-1</sup> to 2226.9 cm<sup>-1</sup>) indicating the electron transfer between S and Au could contribute to the red-shift of the vibrational Stark probe CN. To further verify this conclusion, we repeated the above experiment with ether instead of hexane and Ar stream instead of nitrogen stream to obtain sample spectra that increases the electron transfer between S and Au after removing ether vapor (Fig. S1 in Supporting information). Results as we expected (Fig. 3b, pink line in bottom panel), CN vibration undergoes 0.6 cm<sup>-1</sup> redshift (from 2226.5 cm<sup>-1</sup> to 2225.9 cm<sup>-1</sup>). To further verify the important contribution of electron transfer to the redshift of CN comparing with that in the bulk, MD trajectory analysis was applied to obtain CN vibrational density of states of MBN (Figs. S2 and S3 in Supporting information), which is in good agreement with the experimental result that CN vibration exhibits a more pronounced red shift at interface than in the bulk. As for the mechanism which the electron transfer between S and Au inducing the red-shift of CN in MBN, electron flowing from Au to S increases the electron density of MBN molecule and strengthen the anti-bonding orbitals of CN overlap resulting in the red-shift of CN [34] which is a significant factor why there is a clear red shift of CN vibration in MBN-assembled Au interface than in the bulk. Electron transfer-induced red-shift of CN wavenumber also occurred on other metal interfaces. As reported, the Au/MBN/air system presented CN stretching frequencies around 2226 cm<sup>-1</sup> [13] which is red-shift than Ag/MBN/air system (around 2230 cm<sup>-1</sup>) [13,35,36]. Both of them are red-shifted than gas phase (2238 cm<sup>-1</sup>) [13] which verified the electron transfer from metal to S resulting in the red-shift of CN. The stronger interaction between S atom and Au than Ag [37,38] induced larger electron transfer resulting in lower wavenumber of CN assembly on Au which further confirm the electron transfer-induced red-shift of CN wavenumber.

Since the zero-charge potential of the Au electrode is lower than the open circuit potential (Fig. S4 in Supporting information), Au has a positive surface charge in solution. To reveal the contribution of the interfacial positive electric field to the vibration of CN, salt ions were introduced to shield interfacial electric field and compress the electric double layer (Fig. 4a), which results in a red

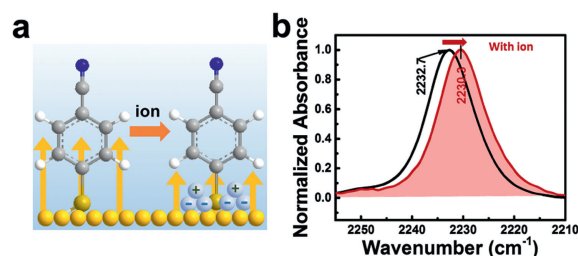


**Fig. 4.** (a) Diagram of MBN in interfacial electric field. (b) SEIRA spectra of MBN in H<sub>2</sub>O with (red line)/without (black line) the addition of 10 mmol/L phosphate buffer solution.

shift of 2.4 cm<sup>-1</sup> (from 2232.7 cm<sup>-1</sup> to 2230.3 cm<sup>-1</sup>) of the band of CN (Fig. 4b), indicating that the positive interfacial electric field induced a blue-shift of the vibration of CN. Whether blue shift or red shift of vibrational probe depends on the direction of the electric field and the electric dipole moment. When the direction of the electric field is parallel to that of the electric dipole moment, the vibrational transition energy from the ground state to the excited state decreases, resulting in the red shift of spectrum. Conversely, antiparallel of the direction of the electric field to the electric dipole moment results in blue shift of the absorption of Stark probe [12]. Thus the potential-induced blue shift of CN vibration is contradictory to the red shift of the assembled CN at Au electrode relative to CN vibration in the bulk, so this is not the dominant cause of the difference between the interface and the bulk.

An accurate and quantitative description of the interface electric field is of great significance for revealing the underlying biological and chemical reaction mechanism, and it is also a great challenge in the study of the interfaces. Revealing the factors that affect the vibrational frequency of Stark probe at interface is a pre-requirement for evaluation the absolute interfacial electric field. Herein, combining SEIRA spectroscopy, ATR spectroscopy and MD calculations, we found solvent electric field, intermolecular  $\pi$ - $\pi$  interaction, electron transfer between S and Au, interfacial electric field all contribute to the vibrational frequency shift of CN. We reveal the assembled C≡N at gold nanofilm exhibits a reduced STR comparing with the bulk which was regulated by the electron transfer between S and Au. Our research lays a foundation for better understanding the interfacial VSE and provides guidance for establishing quantitative model to evaluate the local electric field.

#### Declaration of competing interest

The authors declare that they have no known competing financial interests or personal relationships that could have appeared to influence the work reported in this paper.

#### CRediT authorship contribution statement

**Manyu Zhu:** Formal analysis, Investigation, Methodology, Writing – original draft, Writing – review & editing. **Fei Liang:** Formal analysis, Methodology. **Lie Wu:** Formal analysis, Funding acquisition, Project administration. **Zihao Li:** Formal analysis. **Chen Wang:** Formal analysis. **Shule Liu:** Formal analysis, Methodology. **Xiue Jiang:** Formal analysis, Funding acquisition, Project administration, Writing – original draft, Writing – review & editing.

#### Acknowledgments

We acknowledge The National Key R&D Program of China (No. 2022YFE0113000), the National Science Fund for Distinguished Young Scholars (No. 22025406, the National Natural Science Foundation of China (Nos. 22074138, 12174457) and the

Youth Innovation Promotion Association of CAS (No. 2020233) for financial support.

#### Supplementary materials

Supplementary material associated with this article can be found, in the online version, at doi:10.1016/j.ccl.2024.109962.

#### References

- [1] S. Banerjee, C.S. Gerke, V.S. Thoi, *Acc. Chem. Res.* 55 (2022) 504–515.
- [2] R.E. Warburton, A.V. Soudackov, S. Hammes-Schiffer, *Chem. Rev.* 122 (2022) 10599–10650.
- [3] X. Yu, A. Manthiram, *Energy Environ. Sci.* 11 (2018) 527–543.
- [4] S.M. Lu, Y.Y. Peng, Y.L. Ying, Y.T. Long, *Anal. Chem.* 92 (2020) 5621–5644.
- [5] M.X. Chen, Y. Liu, T.W. Song, et al., *Chin. J. Chem.* 40 (2022) 2161–2168.
- [6] X.Q. Li, G.Y. Duan, X.X. Yang, L.J. Han, B.H. Xu, *Fundam. Res.* 2 (2022) 937–945.
- [7] M.F. Delley, E.M. Nichols, J.M. Mayer, *J. Am. Chem. Soc.* 143 (2021) 10778–10792.
- [8] S. Li, L. Wu, X. Zhang, X. Jiang, *Angew. Chem. Int. Ed.* 59 (2020) 6627–6630.
- [9] R.A. Wong, Y. Yokota, M. Wakisaka, J. Inukai, Y. Kim, *Nat. Commun.* 11 (2020) 4194.
- [10] D. Wright, S. Sangtarash, N.S. Mueller, et al., *J. Phys. Chem. Lett.* 13 (2022) 4905–4911.
- [11] S.S. Andrews, S.G. Boxer, *J. Phys. Chem. A* 104 (2000) 11853–11863.
- [12] S.D. Fried, S.G. Boxer, *Acc. Chem. Res.* 48 (2015) 998–1006.
- [13] G. Schkolnik, J. Salewski, D. Millo, et al., *Int. J. Mol. Sci.* 13 (2012) 7466–7482.
- [14] J.B. Weaver, J. Kozuch, J.M. Kirsh, S.G. Boxer, *J. Am. Chem. Soc.* 17 (2022) 7562–7567.
- [15] D. Bhattacharyya, P.E. Videla, J.M. Palasz, et al., *J. Am. Chem. Soc.* 144 (2022) 14330–14338.
- [16] J.K. Staffa, L. Lorenz, M. Stolarski, et al., *J. Phys. Chem. C* 121 (2017) 22274–22285.
- [17] S.A. Sorenson, J.G. Patrow, J.M. Dawlaty, *J. Am. Chem. Soc.* 139 (2017) 2369–2378.
- [18] X. Chang, H. Xiong, Y. Xu, et al., *Catal. Sci. Technol.* 11 (2021) 6825–6831.
- [19] J. Heo, H. Ahn, J. Won, et al., *Science* 370 (2020) 214–219.
- [20] K. Ataka, T. Kottke, J. Heberle, *Angew. Chem. Int. Ed.* 49 (2010) 5416–5424.
- [21] X.F. Zhang, L. Wu, W.Y. Zhen, et al., *Fundam. Res.* 2 (2022) 66–73.
- [22] F. Zaera, *Chem. Rev.* 112 (2012) 2920–2986.
- [23] D.T. Kwasniewski, H. Wang, Z.D. Schultz, *Chem. Sci.* 6 (2015) 4484–4494.
- [24] A.K. Tewari, R. Dubey, *Bioorg. Med. Chem.* 16 (2008) 126–143.
- [25] V. Chandrasekaran, L. Biennier, E. Arunan, D. Talbi, R. Georges, *J. Phys. Chem. A* 115 (2011) 11263–11268.
- [26] L. Wu, L. Zeng, X. Jiang, *J. Am. Chem. Soc.* 137 (2015) 10052–10055.
- [27] M.O. Sinnokrot, C.D. Sherrill, *J. Phys. Chem. A* 110 (2006) 10656–10668.
- [28] A. Banerjee, A. Saha, B.K. Saha, *Cryst. Growth Des.* 19 (2019) 2245–2252.
- [29] R. Laatikainen, J. Ratilainen, R. Sebastian, H. Santa, *J. Am. Chem. Soc.* 117 (1995) 11006–11010.
- [30] G. Klebe, F. Diederich, *Phil. Trans. R. Soc. Lond. A* 345 (1993) 37–48.
- [31] K. Müller-Dethlefs, P. Hobza, *Chem. Rev.* 100 (2000) 143–168.
- [32] H. Gronbeck, A. Curioni, W. Andreoni, *J. Am. Chem. Soc.* 122 (2000) 3839–3842.
- [33] Y.H. Wang, M.M. Liang, Y.J. Zhang, et al., *Angew. Chem. Int. Ed.* 57 (2018) 11257–11261.
- [34] S. Sarkar, J.G. Patrow, M.J. Voegtle, A.K. Pennathur, J.M. Dawlaty, *J. Phys. Chem. C* 123 (2019) 4926–4937.
- [35] L.J. Huang, D.W. Sun, Z.H. Wu, H.b. Pu, Q.Y. Wei, *Anal. Chim. Acta* 1167 (2021) 338570.
- [36] D. Gkogkou, B. Schreiber, T. Shaykhtudinov, et al., *ACS Sens.* 1 (2016) 318–323.
- [37] K. Fujisawa, S. Imai, Y. Moro-oka, *Chem. Lett.* 2 (1988) 167–168.
- [38] P. Pyykkö, *Angew. Chem. Int. Ed.* 43 (2004) 4412–4456.